


Summer 8-14-2020

## Development of an LC-ESI-MS/MS method for determination of a novel Pyrrolomycin (MP-1) and application to pre-clinical ADME studies

Wafaa N. Aldhafiri  
*University of Nebraska Medical Center*

Tell us how you used this information in this [short survey](#).

Follow this and additional works at: <https://digitalcommons.unmc.edu/etd>

 Part of the [Medicinal and Pharmaceutical Chemistry Commons](#), [Neoplasms Commons](#), [Other Pharmacy and Pharmaceutical Sciences Commons](#), [Pediatrics Commons](#), and the [Pharmacology Commons](#)

---

### Recommended Citation

Aldhafiri, Wafaa N., "Development of an LC-ESI-MS/MS method for determination of a novel Pyrrolomycin (MP-1) and application to pre-clinical ADME studies" (2020). *Theses & Dissertations*. 478.  
<https://digitalcommons.unmc.edu/etd/478>

This Thesis is brought to you for free and open access by the Graduate Studies at DigitalCommons@UNMC. It has been accepted for inclusion in Theses & Dissertations by an authorized administrator of DigitalCommons@UNMC. For more information, please contact [digitalcommons@unmc.edu](mailto:digitalcommons@unmc.edu).

**Development of an LC-ESI-MS/MS method for determination of a novel Pyrrolomycin (MP-1)  
and application to pre-clinical ADME studies**

By

**Wafaa Nasser Aldhafiri**

A THESIS

Presented to the Faculty of  
the University of Nebraska Graduate College  
in Partial Fulfilment of the Requirements  
for the Degree of Master of Sciences

Pharmaceutical Sciences Graduate Program

Under the Supervision of Professors, Daryl J Murry and Rongshi Li

University of Nebraska Medical Center  
Omaha, Nebraska

August 2020

Supervisory Committee:

Anthony T Podany, Pharm.D.

Rongshi Li, Ph.D.

Daryl J Murry, Pharm.D.

## ACKNOWLEDGEMENTS

First and foremost, I want to acknowledge and thank my patient and supportive supervisor Dr. Daryl J Murry for his mentorship and guidance over the course of my master training. He has taught me more than I could ever give him credit for and showed me, by his example, what a good scientist and a person should be.

I extend my abundant gratitude to my thesis co-chair Dr. Rongshi Li and my supervisory committee member Dr. Anthony T Podany. I thank them sincerely for their advice and all the enjoyable discussions we had, which helped to have faith in my own opinion as a scientist.

I am grateful for those with whom I have had the pleasure to work with during this and other related projects, specially Dr. Yashpal Singh Chhonker. I am forever in debt for all the laboratory and research skills he helped me improve and perfect. I am greatly thankful for all the time he rectified my mistakes and slipups before Dr. Murry noticed them.

I am also grateful to the faculty, staff and fellow graduate students in the Pharmaceutical Sciences Graduate Program (PSGP) at University of Nebraska Medical Center (UNMC), with special thanks to Dr. Aaron Mohs, UNMC faculty Senate Vice President, for his guidance and support for all graduate student while he served as PSGP program director. And to Ms. Renee Kaszynski for her willingness to help and extending her warmth and assistance to all students.

I would also like to thank the Saudi Arabian Cultural Mission (SACM), without their financial support of my Master training this work would not have been possible. We also acknowledge financial support from the Fred and Pamela Buffett Cancer Center Support Grant from the National Cancer Institute (P30 CA036727) and the State of Nebraska through the Pediatric Cancer Research Group.

Also, I extend my gratitude for my eternal cheerleaders, the strangers who became as close as family, my friends: Lama, Atheer, Maha and Christin.

Finally, I would like to pay special gratitude, warmth, and appreciation to my family, my parents, Hadwa Shadad and Nasser Aldhafiri, whose love and guidance are with me in whatever I pursue.

اتقدم بخالص الشكر وعظيم الامتنان لوالدتي الفاضلة هدوى شداد الظفيري و لولدي الفاضل ناصر مضحي الظفيري, إني  
مدينه لكم بكل ما وصلت إليه وما أرجو أن أصل إليه من الرفعة و العزه. ولو أنني أوتيت كل بلاغة لشكركم، لما كنت بعد  
القول إلا مقصراً.

I would not have started this journey or have been able to complete it without the love and support of my sisters Abeer, Aljoharah, Bayan, Rawan and Hala Aldhafiri. Thank you for believing in me when I was filled with doubt, for loving me more than I loved my self and for your patience and availability for my long phone calls.

**Development of an LC-ESI-MS/MS method for determination of a novel Pyrrolomycin (MP-1)  
and application to pre-clinical ADME studies**

Wafaa Nasser Aldhafiri, M.S.

University of Nebraska Medical Center, 2020

Supervisor: Daryl J Murry, Pharm.D. and Rongshi Li, Ph.D.

A rapid, selective, and sensitive liquid chromatography coupled with tandem mass spectrometry (LC-MS/MS) method was developed and validated for quantitation of a novel Pyrrolomycin (**MP-1**) in mouse plasma. MP-1 was extracted from plasma utilizing a structural analog (PL-3) as the internal standard (IS). Analyte separation was achieved using a Waters Acquity UPLC®BEH C18 column (1.7  $\mu$ m, 100 x 2.1 mm) protected with Acquity UPLC C18 guard column. Mobile phase consisted of 0.1% acetic acid in water (10%) and methanol (90%) at a total flow rate of 0.25 mL/min. The mass spectrometer was operated at unit resolution in the multiple reaction monitoring (MRM) mode, using precursor ion>product ion transitions of 324.10>168.30 m/z for MP-1 and 411.95>224.15 m/z for PL-3. The MS/MS response was linear over the concentration range from 0.2-500 ng/mL for **MP-1** with a correlation coefficient ( $r^2$ ) of 0.988 or better. Precision (percent relative standard deviation, % RSD) and accuracy (% bias) were within the acceptable limits as per FDA guidelines. MP-1 was stable under storage and laboratory handling conditions. The validated method was successfully applied to assess the solubility, *in vitro* metabolism, plasma protein binding and bio-distribution studies of MP-1. Glucuronidation was found to be the major metabolic pathway using S9 fractions. The validated method was successfully applied to a pre-clinical pharmacokinetic and bio-distribution mouse study involving low volume blood and tissue samples for quantitation of MP-1.

## TABLE OF CONTENTS

### Contents

List of Figures: .....	7
List of Tables: .....	8
List of Abbreviation:.....	9
CHAPTER 1: .....	11
1. Introduction/Background: .....	11
CHAPTER 2: .....	13
2. Materials and methods.....	13
2.1. Chemicals and materials .....	13
2.2. Methods.....	13
2.2.1. Liquid chromatographic and mass spectrometric (LC-MS/MS) conditions for MP-1 .....	13
2.2.2. Preparation of stock, calibration standards and quality control samples .....	14
2.2.3. Plasma, tissue, microsomes, and liver S9 fraction sample preparation .....	15
2.3. Method validation: .....	16
2.3.1. Selectivity and sensitivity.....	16
2.3.2. Calibration curve and linearity.....	16
2.3.3. Carry-over .....	17
2.3.4. Accuracy and precision .....	17
2.3.5. Extraction recovery and matrix effect .....	17
2.3.6. Stability .....	18
2.3.7. Dilution integrity .....	18
2.3.8. Solubility of MP-1.....	19
2.4. In vitro studies: .....	19
2.4.1. Gastrointestinal fluid stability studies of MP-1 .....	19
2.4.2. The blood to plasma ratio (Kb/p).....	19
2.4.3. Plasma Protein Binding (PPB) study.....	20
2.4.4. In vitro Metabolic stability in Mouse S9 Fraction .....	21
2.4.5. In vitro Metabolic stability in mouse, rat, and human liver microsomes .....	22
2.4.6. Metabolite identification .....	23
2.5. In-vivo Pharmacokinetic studies: .....	23
2.5.1. Biodistribution studies animals, drug administration and sampling .....	23
2.5.2. Data analysis .....	24

CHAPTER 3: .....	26
3. Results .....	26
3.1. Chromatographic and mass spectrometric conditions optimization .....	26
3.2. Plasma and tissue sample preparation and liver S9 fraction sample preparation .....	27
3.3. Assay validation .....	27
3.3.1. Selectivity and Sensitivity.....	27
3.3.2. Calibration curve and linearity.....	28
3.3.3. Carry-over .....	28
3.3.4. Accuracy and precision .....	29
3.3.5. Recovery and matrix effect.....	29
3.3.6. Stability .....	30
3.3.7: Dilution integrity .....	32
3.3.8. Solubility of MP-1.....	32
3.4. <i>In vitro</i> studies.....	32
3.4.1. Gastrointestinal Stability of MP-1.....	32
3.4.2. The blood to plasma ratio (Kb/p).....	33
3.4.3. Plasma Protein Binding .....	33
3.4.4. <i>In vitro</i> metabolic stability in microsomes.....	33
3.4.5. <i>In vitro</i> Metabolic stability in Mouse S9 Fraction .....	34
3.4.6. Metabolite identification .....	35
3.5. <i>In vivo</i> pharmacokinetic studies.....	38
3.5.1. Pharmacokinetic study.....	38
3.5.2. Tissue distribution study .....	40
CHAPTER 4: .....	42
4.1. Discussion.....	42
4.2. Study limitations and future directions .....	43
5. Conclusion:.....	44
6. Bibliography .....	45

## List of Figures:

<b>Figure 1: Representative MRM ion-chromatograms.</b> (a) Blank mouse plasma using the conditions for MP-1 detection, (b) MP-1 spiked in mouse plasma at LQC 0.6 ng/mL, (c) mouse Plasma from pre-clinical study sample at 0.5 hr time point showing MP-1, (d) blank plasma using the conditions for PL-3 detection, (e) PL-3 spiked in plasma 0.5 ug/mL, (f) plasma from pre-clinical study sample at 0.5 hr time point spiked with IS showing PL-3.....	26
<b>Figure 2: MP-1 calibration curve and linearity.</b> Linear calibration fit for MP-1 of concentration range of 0.2 to 500 ng/mL, $r^2 = 0.988$ and %RSD= 9.97.....	28
<b>Figure 3: Gastrointestinal Stability of MP-1.</b> MP-1 stability following a 2 hr incubation in buffer pH 7.4, SIF pH 6.8, SGF pH 1.2. ....	32
<b>Figure 4: Figure 4: MP-1 In vitro metabolic stability in microsomes.</b> Time-dependent metabolic depletion (% turnover or amount of drug remaining vs. incubation time) of MP-1 in microsomes and mouse S9 fraction (a) Interspecies microsomal metabolic stability of MP-1 in presence of NADPH and absence of NADPH as a negative control (b) mouse S9 metabolic stability of MP-1 in presence of NADPH and absence of NADPH as a negative control. Data shown as mean $\pm$ S.D (n=3).....	34
<b>Figure 5: MP-1 Metabolite identification.</b> Representative overly chromatogram of MP-1 and its metabolites under 35 min gradient chromatography. ....	36
<b>Figure 6: MP-1 metabolites chromatogram:</b> a) Precursor ion spectra of MP-1 b) MP-1 metabolite in negative ESI mode, [M-H] <sup>-</sup> 324.10 and 500.10, respectively. ....	37
<b>Figure 7: The blood concentration vs. time profile for the MP-1.</b> Plasma concentration-time profile after 15mg/kg oral administration of MP-1 (Mean $\pm$ S.D, n=4).....	38
<b>Figure 8: MP-1 tissues concentrations.</b> Tissue concentrations (ng/g) at different time points in liver, lungs, heart, kidney, brain, and spleen after 15mg/kg oral administration of MP-1 in mice (Mean $\pm$ S.D, n=4). ....	41



## List of Tables:

<b>Table 1: Summary of MS/MS parameters:</b> precursor ion, fragment ions, voltage potential (Q1), collision energy (CE) and voltage potential (Q3) for MP-1 and IS.....	14
<b>Table 2: MP-1 accuracy and precision.</b> Intra–assay and inter–assay accuracy and precision of MP-1 in plasma (n = 6).....	29
<b>Table 3: Recovery and matrix effect.</b> Assessment of the recovery and matrix effect of MP-1 in mouse plasma, (Mean ± S.D, n=3). ....	30
<b>Table 4: Stability of MP-1.</b> stability was tested in mouse plasma at different storage conditions, (Mean ± S.D, n=3). ....	31
<b>Table 5: The value MP-1 the blood to plasma ratio (Kb/p).</b> MP-1 concentration in blood and plasma, (Mean ± S.D, n=3).....	33
<b>Table 6: MP-1 Plasma Protein Binding.</b> Plasma protein binding in mouse plasma (Mean ± S.D values for MP-1, n=3). ....	33
<b>Table 7: <i>In vitro</i> Metabolic stability in Mouse S9 Fraction.</b> MP-1 estimates for CL <sub>int</sub> , t <sub>1/2</sub> and CL <sub>int,H</sub> in mouse (MLM) , rat (RLM) and human (HLM) liver microsomes, and mouse S9, (Mean ± S.D, n=3). ....	35
<b>Table 8: MP-1 metabolites chromatogram summary.</b> MP-1 metabolites biotransformation, mass shift, precursor ion and retention time. ....	36
<b>Table 9: MP-1 Plasma concentration,</b> after 15 mg/kg oral administration in mice (Mean ± S.D, n=4). ....	39
<b>Table 10: Summary of MP-1 pharmacokinetic parameters,</b> Non-compartmental pharmacokinetic parameters of MP-1 after 15 mg/kg oral administration (Mean, S.D SE and CV%, n=4). ....	39
<b>Table 11: MP-1 tissues concentrations.</b> Tissue concentrations (ng/g) in liver, lungs, heart, kidney, brain, and spleen after 15mg/kg oral administration of MP-1 in mice (Mean ± S.D, n=4). ....	40

**List of Abbreviation:**

- (NB)** Neuroblastoma
- (OXPHOS)** Oxidative phosphorylation
- (ATP)** Adenosine triphosphate
- (LC-MS/MS)** Liquid chromatographic and mass spectrometric
- (ESI-)** Negative ionization electrospray ionization mode
- (DL)** Desolvation line
- (MRM)** Multiple reaction monitoring
- (IS)** Internal standard
- (CS)** Calibration standards
- (QCs)** Quality control samples
- (MeOH)** Methanol
- (LLOQ)** Lower limit of quantification
- (LQC)** Low quality control
- (MQC)** Middle quality control
- (HQC)** High quality control
- (ACN)** Acetonitrile
- (% R.S.D)** Relative standard deviation
- (ME)** Matrix effect
- (Kp)** Blood concentration ratio
- (C<sub>max</sub>)** Peak plasma concentration
- (T<sub>max</sub>)** Time for the peak plasma concentration
- (AUC<sub>0-∞</sub>)** The area under the curve
- (t<sub>1/2</sub>)** The elimination half-life
- (CL)** Clearance
- (r<sup>2</sup>)** Correlation coefficient of determination

**(V<sub>d</sub>)** Volume of distribution

**(SD)** Standard deviation

**(CV)** Coefficient of variation

**(IE)** Ionization efficiency

**(LLOD)** The lower limit of detection

**(ULOQ)** Upper limit of quantification

## **CHAPTER 1:**

### **1. Introduction/Background:**

Neuroblastoma (NB) is a rare embryological malignancy derived from neural crest cells. The neural crest is a group of neuronal cells that migrate from the spinal cord to form many structures during fetal development. NB is mainly diagnosed before the age of 5 years, with a median age of diagnosis of 18 months. Approximately 800 children are diagnosed with NB each year in the United States, making it the second most common extracranial malignant tumor of childhood and the most common solid tumor of infancy. Moreover, NB accounts for approximately 15% of pediatric cancer deaths [1-4].

Neuroblastoma is characterized by being one of the most enigmatic pediatric tumors with high clinical heterogeneity behavior due to a prognosis that varies widely, from tumors that spontaneously regress and require no intervention to those that present with metastatic disease. Approximately 60% of children diagnosed with NB have metastatic disease at diagnosis and have resistant disease to conventional therapy resulting in poor survival[1, 3, 5].

Several genetic alterations have been observed in NB cells, including amplification of MYCN, which is present in approximately 40% of high-risk NB patients. MYCN amplification is associated with a poor survival rate of only 14–34%, even in patients with favorable outcome profiles[6, 7]. Amplification of MYCN supports oxidative glycolysis, also known as the Warburg effect, by activating the transcription of several glycolytic genes to meet the NB cells elevated need for glucose. Inhibition of MYCN pathways may lead to autophagy, quiescence and cell death and be a novel target for drug therapy of NB[4, 8]. Despite advances in therapy, treatment of pediatric neuroblastoma with MYCN amplification remains challenging [9]. There is a critical need to identify agents that target the MYCN pathway and improve outcomes in pediatric NB.

Marinopyrroles were first reported as a promising antibiotic agent, however recent studies have identified these compounds to have anti-myeloid cell leukemia 1 (Mcl-1) activity, suggesting they have anticancer activity. Mcl-1 is an anti-apoptotic protein, highly expressed in a variety of human cancers and a validated drug target for cancer treatment[10, 11]. Although marinopyrroles might represent a new class of anticancer compounds, their physicochemical and drug-like properties are not ideal for drug development. The majority of marinopyrroles have poor solubility, limiting enthusiasm for further development to an orally active drug. Marinopyrroles with improved physicochemical and drug-like properties have recently been described [8]. Moreover, a novel marrinopyrrole derivative, MP-1, has been shown to have activity in a resistant neuroblastoma cell line overexpressing MYCN by inhibiting MYCN and MCL-1, while stimulating autophagy and inhibition of oxidative phosphorylation (OXPHOS) metabolism [8].

In order to characterize *in vitro* properties and assess the pharmacokinetics and biodistribution of MP-1, we developed a rapid and sensitive bioanalytical method for the quantification of MP-1 with a short run time (~6 min). The results of these studies provide the needed information to guide MP-1 dosing in animal models of NB. Further, these findings in correlation with biological response will be useful for further evaluation of the therapeutic use of MP-1.

## **CHAPTER 2:**

### **2. Materials and methods**

#### **2.1. Chemicals and materials**

MP-1 (purity:  $\geq 98\%$ ) and PL-3 (purity:  $\geq 99.9\%$ ), used as an internal standard (IS), were generously provided by Dr. Rongshi Li (UNMC). Methanol (MeOH), acetonitrile (ACN) and sodium acetate were purchased from Fisher Scientific (Fair Lawn, NJ). All solvents were HPLC grade or higher. Water was purified using a Barnstead GenPure water purification system (ThermoScientific, Waltham, MA). Bond Elute C18 cartridges (50 mg per 1 mL) were purchased from Agilent (Agilent Inc., Santa Clara, CA). Mouse blood and plasma was purchased from Equitech-Bio, Inc. (Kerrville, Texas). All other materials and reagents that was used in this paper were purchased from standard chemical suppliers and of analytical grade or higher.

#### **2.2. Methods**

##### **2.2.1. Liquid chromatographic and mass spectrometric (LC-MS/MS) conditions for MP-1**

An LC-MS/MS 8060 system (Shimadzu Scientific Instruments, Columbia, MD) equipped with a dual ion source (DUIS), was used to perform mass spectrometric detection. LabSolutions LCMS software Version 5.8 (Shimadzu Scientific, Inc., Columbia, MD) was used for data acquisition and quantitation. To achieve the desired sensitivity, the compound dependent mass spectrometer parameters, such as temperature, voltage, gas pressure, etc., were optimized by auto method optimization via product ion search for MP-1 and PL-3 as internal standard (IS) using a 0.5  $\mu\text{g/mL}$  solution in methanol. All analytes were detected in the negative ionization mode utilizing electrospray ionization (ESI<sup>-</sup>) with the mass spectrometer source settings as follows: nebulizer gas: 2.0 L/min; drying gas: 10 L/min; heating gas: 10 L/min; interface temperature: 300 °C; desolvation line (DL) temperature: 250 °C; heat block temperature: 400 °C. The MS/MS system was operated at unit resolution in the multiple reaction monitoring (MRM) mode, using

precursor ion>product ion combinations of 324.10>168.30 m/z for MP-1 and 411.95>224.15 m/z for PL-3, IS, results are shown in Table 1. along with their respective optimum MS parameters.

Analytes	MRM transition m/z (Q1→Q3)	Q1 (V)	Q3 (V)	CE (V)	Retention time (min)
Target: MP-1	324.10>168.30	-11	-10	-22	1.9
	324.10>304.30	-11	-20	-18	
Internal standard (IS): PL-13	411.94>224.14	-14	-14	-28	4.5

**Table 1: Summary of MS/MS parameters:** precursor ion, fragment ions, voltage potential (Q1), collision energy (CE) and voltage potential (Q3) for MP-1 and IS.

All chromatographic separations were performed with an Acquity UPLC®BEH C18 column (1.7µm, 100 x 2.1 mm, Waters, Inc. Milford MA) equipped with an Acquity UPLC C18 guard column (Waters, Inc. Milford MA). The mobile phase consisted of 0.1% acetic acid in water (mobile phase A) and methanol (MeOH) (mobile phase B) operated in isocratic mode with 10% A and 90% B with a total flow rate of 0.25 mL/min. The total run time was 6 minutes. The injection volume of all samples was 2 µL.

### 2.2.2. Preparation of stock, calibration standards and quality control samples

Stock solutions of MP-1 and IS were prepared at 1 mg/mL concentrations in DMSO. The stock solutions were diluted with MeOH to make working standard solutions and used to prepare the calibration standards (CSs) and quality control samples (QCs). CSs and QCs were prepared by spiking 10 µL of working standard solution and 10 µL of IS working solution (0.5 µg/mL) into 100 µL of blank mouse plasma or tissue homogenate to obtain a concentration range of 0.2–500 ng/mL. The obtained CS concentrations were: 0.2, 0.5, 1, 5, 10, 50, 200 and 500 ng/mL in bio-matrices. The QCs comprised four concentrations: 0.2 ng/mL - the lower limit of quantification

(LLOQ), 0.6 ng/mL - low quality control (LQC), 100 ng/mL - middle quality control (MQC), and 375 ng/mL - high quality control (HQC). QCs were prepared separately in five replicates, independent of the calibration standards. CSs and QCs were freshly prepared prior to use and all the main stocks, intermediate stocks, spiking calibration, and QC stock solutions were kept at -20 °C.

### **2.2.3. Plasma, tissue, microsomes, and liver S9 fraction sample preparation**

All analytes were extracted from CSs, QCs, mouse blood, and tissue samples by solid-phase extraction (SPE) using Agilent bond Elute C18 cartridges. Samples were prepared by spiking 100 µL of appropriate calibration stock in 100 µL blank bio-matrix (blank mouse plasma or tissue homogenate) and 10 µL of IS solution (0.5 µg/mL) and further diluted with 1% acetic acid (600 µL). A Cerex solid-phase extraction manifold from Varian (Palo Alto, CA) with nitrogen to modulate flow was used for sample processing. Samples were vortexed for 2 minutes and then loaded onto SPE cartridges pre-conditioned with MeOH (2 mL), followed by water (1 mL). Loaded cartridges were washed with 15% MeOH (1 mL) and eluted with MeOH (2 mL). The eluate was evaporated under vacuum at room temperature then reconstituted in 200 µL of mobile phase (10:90; 0.1% AA : MeOH) then vortexed for 30 seconds and centrifuged at 13,400 x g for 10 min at 4 °C, and the supernatant transferred to HPLC vial for injection and analysis.

Each tissue sample was accurately weighed and then homogenized with de-ionized water at a 5- fold dilution factor for liver, spleen, brain, lungs, and kidney using a TissueLyserII (Qiagen Science, KY). Heart tissue was homogenized at a 6-fold dilution factor. The resultant tissue homogenate (100 µL) was spiked with 10 µL of IS solution and prepared for solid-phase extraction as describe above for plasma samples.



S9 fraction and microsomal incubation buffer samples were extracted using simple protein precipitation. S9 fraction samples (100  $\mu$ L) were obtained and mixed with 300  $\mu$ L of ice-cold ACN spiked with 10  $\mu$ L of IS (0.5  $\mu$ g/mL) in a 1.5 mL-centrifuge tube. The samples were vortexed for 2 minutes, then centrifuged 17,940 g for 10 minutes. A 100  $\mu$ L aliquot of the clear supernatant was transferred to an HPLC vial and 2  $\mu$ L injected into the LC-MS/MS system.

### **2.3. Method validation**

The LC–MS/MS method was validated in accordance with guidelines for Bioanalytical Method Validation published by the US-Food and Drug Administration (FDA) [12] with respect to selectivity, specificity, linearity, accuracy, precision, matrix effect, stability, and dilution response.

#### **2.3.1. Selectivity and sensitivity**

Assay selectivity and specificity was determined by comparing the chromatogram of six different blank mouse plasma or tissue homogenate samples with that MP-1 and IS-spiked plasma or tissue homogenate samples. Peak interference at the retention time of analytes and internal standard was investigated by comparing analyte response of interference-free blank plasma, plasma spiked with MP-1 and the IS, and neat stock solutions in reconstitution solvent as described in section 2.2.3.

The sensitivity of the method was determined from the signal-to-noise ratio (S/N) of the response of MP-1 to blank matrix. The S/N ratio was calculated by comparing the baseline noise at the vicinity of the retention time of analyte with that of the LLOQ peak response. The lower limit of detection (LLOD) and LLOQ were defined as a three and ten-fold S/N ratio, respectively.

#### **2.3.2. Calibration curve and linearity**

The calibration curves were established by a linear plot of the relation between the peak area ratio (MP-1/IS) on the y-axis versus concentration of MP-1 on the x-axis. The calibration

curve was generated using weighted linear regression (1/x<sup>2</sup>). Each calibration curve consisted of a blank sample, a zero sample (blank + IS), and 12 non-zero concentrations consisting of eight CS and four QC. The acceptance criteria for each CS concentration was ± 15% standard deviation (SD) from the nominal value except at LLOQ, which was set at ± 20%. The calibration curve had to have a correlation coefficient (r<sup>2</sup>) of 0.988 or better for MP-1. The assay was linear over the range of 0.2 – 500 ng/mL.

### **2.3.3. Carry-over**

Residual carry-over was assessed by injecting two consecutive “zero samples” after running the HQC (375 ng/mL). The response of the first zero sample was required to be <20% of the response of a processed LLOQ sample to conclude no carry-over.

### **2.3.4. Accuracy and precision**

Intra–and inter–assay accuracy and precision were evaluated by analyzing five replicates of QC samples at four different concentrations (LLOQ, LQC, MQC, and HQC) in mouse plasma or tissue homogenate for three consecutive days. Precision was defined as the percent relative standard deviation (%RSD) with acceptance criteria of ± 15% (except ± 20% at LLOQ). Accuracy was defined as the percent bias (% Bias) with the same acceptance criteria as precision. %bias was calculated according to the following Equation 1:

$$\% \text{Bias} = \frac{(\text{observed conc.} - \text{nominal conc.})}{\text{nominal conc}} \times 100 \quad \text{Equation 1}$$

### **2.3.5. Extraction recovery and matrix effect**

Extraction recovery was calculated at three different QC concentrations (LQC 0.2 ng/mL), (MQC 100 ng/mL) and (HQC 375 ng/mL) for both MP-1 and IS (0.5 µg/mL) by comparing the mean peak area of an analyte spiked before extraction to the mean peak area of an analyte spiked post-extraction multiplied by 100.

To assess the effect of the matrix on analyte response, blank mouse plasma and tissue homogenate were processed, the dry post-extract was spiked with analyte prepared equivalent to the QCs. The average peak area from analytes spiked in the extracted blank matrix was compared to the response for QCs prepared in reconstitution solvent. The absolute matrix effect (ME) and IS normalized ME were calculated as described in Equation (2) and (3).

$$ME = \frac{\text{Mean Peak area of analyte spiked post-extraction}}{\text{Mean Peak area of analyte in Solvent}} \times 100 \quad \text{Equation (2)}$$

$$IS \text{ normalized ME} = \frac{\text{Mean Peak area ratio of analyte/IS spiked post-extraction}}{\text{Mean Peak area ratio of analyte/IS in Solvent}} \times 100$$

Equation (3)

### 2.3.6. Stability

Storage stability of MP-1 in mouse plasma samples was determined at three different QC concentrations. The following stabilities were evaluated: bench-top storage (4 h at room temperature 21 °C), three freeze-thaw cycles (-80 °C to room temperature for 30 min, back to -80 °C, stored for 24 h, and repeated twice more), and long-term storage (12 months at -80 °C). Additionally, 24 h auto-sampler stability of extracted samples (at 4 °C) was determined. The sample concentration for MP-1 under each condition was tested and mean values for accuracy and precision calculated.

### 2.3.7. Dilution integrity

The dilution integrity of samples was tested on six replicates of three levels of dilution: two- (2× HQC), five- (5× HQC), and ten-fold (10× HQC) dilutions of the high QC concentration. The calculated concentration measurements were compared to the nominal concentration at each dilution level.

### **2.3.8. Solubility of MP-1**

The solubility of MP-1 was assessed by spiking 1% DMSO stock solutions (5  $\mu$ L) into 100 mM phosphate buffered saline (pH 7.4, 445  $\mu$ L) in triplicate to produce final assay concentrations of 1, 5, 10, 20, 40, 50, 60, 80  $\mu$ M. Spiked samples were kept at room temperature for 2 h. At pre-determined times, each microcentrifuge tube was centrifuged at 10,000 g for 15 min. Supernatant was aspirated and mixed with equal volume of acetonitrile. Calibration curve samples were prepared in buffer, acetonitrile, DMSO media for analysis. Solubility concentration was calculated via the calibration curve using analyte/IS peak area ratio and concentration at which the analyte precipitated out, which was considered as the upper soluble concentration.

## **2.4. In vitro studies**

### **2.4.1. Gastrointestinal fluid stability studies of MP-1**

Simulated gastrointestinal fluids were prepared according to USP specifications. Briefly, simulated gastric fluid (SGF) was formulated consisting of sodium chloride (0.2 g), pepsin (3.2 g), hydrochloric acid (7 mL) in water (1 L, pH 1.2). Simulated intestinal fluid (SIF) was formulated with potassium dihydrogen phosphate (6.805 g), sodium hydroxide (0.896 g), pancreatin (10 g) in water (1 L, pH 6.8). MP-1 at 10  $\mu$ M concentration was incubated with SGF, SIF and phosphate buffer (100mM, pH 7.4) at 37 °C on a shaking water bath each in triplicate. Samples (200  $\mu$ L) were collected at 0, 15, 30, 60 and 120 min. Immediately after sample collection, five volumes of MeOH containing IS were added and samples prepared for analysis. Stability was determined as a percentage parent compound detected at each time point relative to the concentration at 0 min in buffer (100%)[13].

### **2.4.2. The blood to plasma ratio (Kb/p)**

The mouse blood to plasma partitioning of MP-1 was determined at concentrations of 1  $\mu$ M. Fresh mouse blood (800  $\mu$ L) was incubated in a water bath maintained at 37 °C for 10 min. After

incubation, blood was spiked with the drug from stock solutions of 1  $\mu\text{M}$  (325 ng/mL) to achieve final concentrations and to maintain organic content <1%. At different time points (0, 30, 60min), aliquots (50  $\mu\text{L}$ ) were collected for blood analysis and an additional sample (120  $\mu\text{L}$ ) was transferred into a micro centrifuge tube and centrifuged at 4000 g for 10 min at 4  $^{\circ}\text{C}$  to separate 50  $\mu\text{L}$  plasma for analysis. Blank plasma (50  $\mu\text{L}$ ) was added to the blood aliquot, and 50  $\mu\text{L}$  of blank blood was added to the separated plasma for matrix match and calibration in 100  $\mu\text{L}$ . The whole blood and plasma samples were further processed by SPE as described above. The analyte peak areas ratios were used to calculate the blood-to-plasma (B/P) ratio using Equation 4.

$$B/P \text{ Ratio} = \frac{\text{Analyte Concentration in whole blood}}{\text{Analyte Concentration in Plasma}} \text{ Equation (4)}$$

#### **2.4.3. Plasma Protein Binding (PPB) study**

A Rapid Equilibrium Dialysis (RED) device system (Thermo Scientific, Rockford IL) was used to evaluate PPB by adding buffer to the buffer chamber and dosing solution to the sample chamber. The buffer chamber contained 350  $\mu\text{L}$  of phosphate-buffered saline (containing 100 mM sodium phosphate and 140 mM sodium chloride, pH 7.4). The sample contained mouse plasma spiked with 1  $\mu\text{M}$  or 10  $\mu\text{M}$  MP-1 and was added to the sample chamber. The RED kit top was then sealed and incubated at 37  $^{\circ}\text{C}$  on an orbital shaker at 100 rpm for 5 h.

Plasma stability of MP-1 was assessed along with the non-specific binding potential of MP-1 to the dialysis membrane and cell chambers by spiking drug into buffer while incubating at 37  $^{\circ}\text{C}$  for 5 h and comparing it with 0 h concentration. At pre-determined times, aliquots (40  $\mu\text{L}$ ) were removed from the sample and buffer chambers and mixed with an equal volume of buffer or blank plasma, respectively. The samples were further processed by SPE as described above and analyzed

by LC-MS/MS. The stability, equilibrium, device recovery and PPB were calculated using following equations [14].

$$\% \text{ Remaining at } 5 \text{ h} = \frac{\text{Concentration}_{4 \text{ h}}}{\text{Concentration}_{0 \text{ h}}} \times 100 \text{ Equation (5)}$$

$$\% \text{ Equilibrium} = \frac{\text{Concentration}_{\text{receiver cell}}}{\text{Concentration}_{\text{donor cell}}} \times 100 \text{ Equation (6)}$$

$$\% \text{ Device Recovery} = \frac{\text{Concentration}_{\text{receiver cell}} + \text{Concentration}_{\text{donor cell}}}{\text{Concentration}_{4 \text{ h}}} \times 100 \text{ Equation (7)}$$

$$\% \text{ Bound} = \frac{\text{Concentration}_{\text{donor cell}} - \text{Concentration}_{\text{receiver cell}}}{\text{Concentration}_{\text{donor cell}}} \times 100 \text{ Equation (8)}$$

#### 2.4.4. In vitro Metabolic stability in Mouse S9 Fraction

*in vitro* phase I and II metabolism was assessed using mouse liver S9 fractions (XenoTech, LLC, Lenexa, KS, USA). Briefly, 1  $\mu\text{M}$  MP-1 was pre-mixed with a solution mixture of potassium phosphate buffer (100 mM, pH 7.4) at 37 °C containing the following: 1 mM NADPH, 4 mM saccharolactone, 1 mM uridine 4'-diphospho-glucuronic acid, and 0.1 mM 3'-phosphoadenosin-4'-phosphosulphate. Incubation was performed in triplicate, n=3. Reactions were performed at a final incubation volume of 1000  $\mu\text{L}$  and initiated with the addition of the S9 fraction, 50  $\mu\text{L}$  of 20 mg/mL protein concentration. Immediately after mixing the MP-1 into the incubation mixture, a sampling point was taken, representing t = 0. Subsequent sampling points were performed at the following intervals: 5, 15, 20, 30, 45, 60, 90 and 120 min. To stop the reaction, 100  $\mu\text{L}$  of the sample were added to 1.5 mL-centrifuge tube containing 300  $\mu\text{L}$  of ice-cold ACN spiked with 10  $\mu\text{L}$  of IS (0.5  $\mu\text{g}/\text{mL}$ ). All the samples were vortexed and centrifuged at 13,000 x g for 10 min. The resultant

supernatant was transferred to an autosampler vial and 2  $\mu\text{L}$  injected on the LC-MS/MS. Testosterone, 7-HC and diclofenac were utilized as positive controls to ensuring proper incubation conditions were maintained.

#### **2.4.5. In vitro Metabolic stability in mouse, rat, and human liver microsomes**

Metabolic stability was assessed using mouse, rat, and human liver microsomes (XenoTech, LLC, Lenexa, KS, USA) for phase I metabolism. Briefly, the buffer solution was prepared containing potassium phosphate buffer (100 mM, pH 7.4), 25  $\mu\text{L}$  of microsomal protein (20 mg/mL), magnesium chloride (10 mM) and NADPH (2mM) in a final volume of 0.5 mL was pre-incubated at 37 °C for 10 min in water bath maintaining at 60 rpm. The reaction was started by adding 2 $\mu\text{L}$  of MP-1 (1  $\mu\text{M}$ ). Serial samples (50  $\mu\text{L}$ ) were collected at selected time intervals (0, 5, 15, 20, 30, 45 and 60 min) and quenched with 200  $\mu\text{L}$  of acetonitrile spiked with 10  $\mu\text{L}$  of IS (0.5  $\mu\text{g}/\text{mL}$ ). All the samples were vortexed and centrifuged at 13,000 g for 15 min, supernatant collected and transferred to an autosampler vial and injected (2  $\mu\text{L}$ ) onto the LC-MS/MS system. Testosterone, and diclofenac were used as positive controls to ensure that HLM and incubation conditions were appropriate to conduct metabolism studies.

Both the S9 Fraction and HLM metabolic stability was expressed as the percentage of drug remaining at each time point. The *in vitro* metabolic elimination rate constant was calculated from the first-order plot of a natural logarithm of the area ratio versus time. The slope of the linear regression equation was used to determine elimination rate constant “k” ( $\text{min}^{-1}$ ). The half-life ( $t_{1/2}$ ) was calculated using Equation 9. The *in vitro* intrinsic clearance ( $\text{CL}_{\text{int}}$ ) was determined by using Equation 10. The intrinsic clearance was further extrapolate to *in vitro* hepatic clearance ( $\text{CL}_{\text{int},\text{H}}$ : mL/min/kg of body weight) using a scaling factors and Equation 11 [15, 16].

$$t^{1/2} = 0.693/k \quad \text{Equation (9)}$$

$$CL_{int} = \frac{0.693}{t^{1/2}} \times \frac{\text{Volume of reaction mixture (mL)}}{\text{mg of protein}} \quad \text{Equation (10)}$$

$$CL_{int,H} = CL_{int} \times \frac{\text{mg of protein}}{\text{gram of liver}} \times \frac{\text{gram of liver}}{\text{kg of body weight}} \quad \text{Equation (11)}$$

#### 2.4.6. Metabolite identification

To identify MP-1 metabolites, we performed a mass shift analyses using the same LC-MS/MS system. A 35 min gradient time profile was used for metabolite identification via Q1 scan mode, which ranged of 250 to 1000 Da. The gradient profile of the mobile phase was held at 10% mobile phase B (MeOH) for 1 min then increased up to 95% mobile phase B over 28 minutes, then brought back to 10% B over 1 min, followed by a 4 min equilibration. The parent drug MS/MS spectrum was used as a template model for metabolites structural identification and assuming the fragmentation pattern of the parent drug, MP-1, from the product-ion spectrum, which was used to deduce the structures of the metabolites [17, 18]. The data acquisition for metabolite identification study was conducted using LabSolutions, version 5.8.

### 2.5. In-vivo Pharmacokinetic studies

#### 2.5.1. Biodistribution studies animals, drug administration and sampling

The University of Nebraska Medical Center Institutional Animal Ethics Committee approved all animal studies (protocol number 17-046-06-FC). Female BALB/c mice, with weights ranging from 24 to 30 grams were used for biodistribution studies. Animals were housed in the University of Nebraska Medical Center animal facility, for at least 7 days prior to the experiments, in order to acclimatize the animals to the laboratory conditions, at a temperature of 23–24 °C, relative humidity of 40–70% and 12/12 h light/dark cycles. The dosing solution was



made of DMSO-Polyethylene glycol 400 (PEG400)-Propylene glycol (PG)-EtOH-Cremophore-PBS (2/20/10/10/5/53 % v/v). MP-1 (15 mg/kg) was administered by oral gavage, the dose was selected based on previous pharmacological reports in mice[8]. After dosing, approximately 100  $\mu$ L of blood was collected, in polypropylene tube, from the maxillary vein at 5, 15, 30 minutes and 1, 2, 4, 6, 8, 24, 48 hr. Two blood time points was collected from every mouse and third time point was the terminal time point, for a total of three-time points from each mouse (5 mice/ group/ per time point). Plasma was prepared by centrifugation at 4,000 x g at 4 °C for 10 minutes. The collected plasma samples were stored at -80 °C until analysis.

Tissues (liver, lungs, heart, kidney, brain, and spleen) were collected at 2, 4, 8- and 48-hours following dosing. Tissue samples were rinsed with phosphate buffered saline to remove blood and then blotted with filter paper. After weighing, each tissue sample was individually homogenized with de-ionized water, 5-dilution factor for liver, spleen, brain, lungs and kidney while the heart was homogenized at a 6-dilution factor using a TissueLyser II (Qiagen Science, KY) then all tissues were stored at -80 °C until analysis. Plasma concentrations (ng/mL) and tissue concentrations (ng/g) were determined for each time point collected. Drug accumulation in tissue was determined by calculating a tissue to plasma concentration ratio (Kp) for each tissue.

### **2.5.2. Data analysis**

Non-compartmental pharmacokinetics analysis was performed on Phoenix® 8.2 (Certara Corporation, Mountain View, CA) to determine plasma pharmacokinetic parameter of MP-1 in plasma. Peak plasma concentration ( $C_{max}$ ) and time for the peak plasma concentration ( $T_{max}$ ) was obtained from visual inspection of the concentration-time plot. The area under the curve ( $AUC_{0-\infty}$ ) was estimated using the linear trapezoidal method from 0- $t_{last}$  and extrapolation from last

time point to infinity based on the observed concentration at the last time point divided by the terminal elimination rate constant (k).

The elimination half-life ( $t_{1/2}$ ) was calculated using Equation 12. Clearance (CL) was calculated using Equation 13 and the apparent volume of distribution of the elimination phase ( $V_d$ ) were calculated using Equation 14 The tissue to blood ( $K_p$ ) ratio was calculated by using Equation 15.

$$t_{\frac{1}{2}} = \frac{0.693}{k} \quad \text{Equation (12)}$$

$$CL = \frac{\text{Dose} \left(\frac{mg}{kg}\right)}{AUC_{0-\infty}} \quad \text{Equation (13)}$$

$$V_d = \frac{\text{Dose} \left(\frac{mg}{kg}\right)}{K * AUC_{0-\infty}} \quad \text{Equation (14)}$$

$$K_p = \frac{\text{Concentration in Tissue}}{\text{Concentration in Blood}} \quad \text{Equation (15)}$$

## CHAPTER 3:

### 3. Results

#### 3.1. Chromatographic and mass spectrometric conditions optimization

To optimize MS/MS conditions for MP-1 and IS detection, ESI and atmospheric pressure chemical ionization (APCI) conditions were tested. Signal intensities of MP-1 and the IS were found to be the highest using ESI in the negative ion mode (ESI<sup>-</sup>) (data not shown). MS/MS conditions were optimized using 1 µg/mL of MP-1. De-protonated molecules [M-H]<sup>-</sup> of MP-1 were seen in abundance having a precursor ion>product ion combinations of 324.10>168.30 m/z and 411.95>224.15 m/z for PL-3, respectively (Figure2).

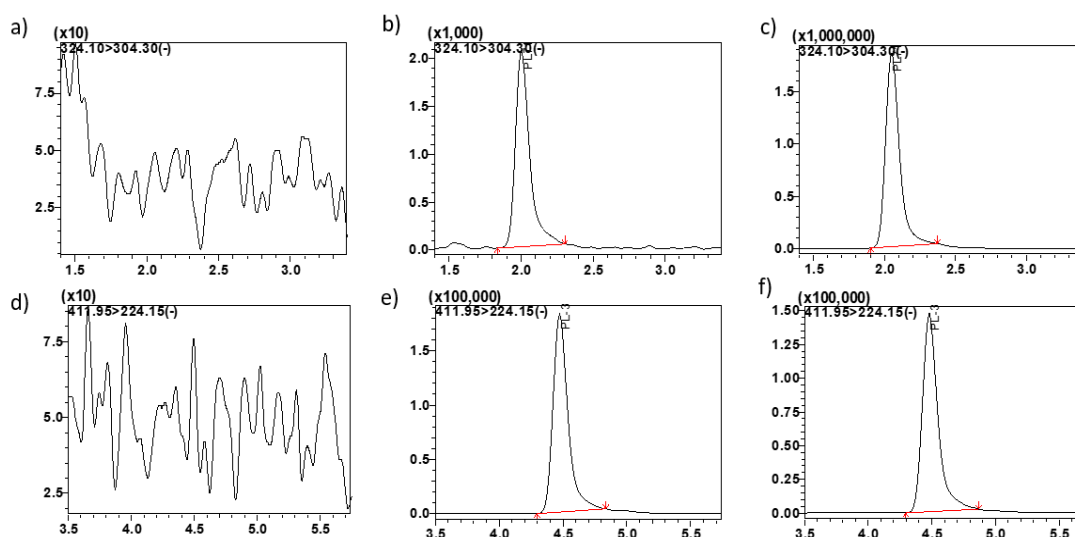


**Figure 1: Representative MRM ion-chromatograms.** (a) Blank mouse plasma using the conditions for MP-1 detection, (b) MP-1 spiked in mouse plasma at LQC 0.6 ng/mL, (c) mouse Plasma from pre-clinical study sample at 0.5 hr time point showing MP-1, (d) blank plasma using the conditions for PL-3 detection, (e) PL-3 spiked in plasma 0.5 µg/mL, (f) plasma from pre-clinical study sample at 0.5 hr time point spiked with IS showing PL-3.

In order to attain short retention times and maximal peak resolution, various chromatographic conditions were investigated including: mobile phase (acetonitrile, MeOH, and water), additives (acetic acid, ammonium acetate, formic acid, and ammonium format), gradient parameters, and analytical columns (C8, C18, and C18 PFP). Final separation conditions were

achieved on an Acquity UPLC®BEH C18 column, 1.7µm, 100 x 2.1 mm, Waters, Inc. Milford MA) column equipped with an Acquity UPLC C18 guard column (Waters, Inc. Milford). Final mobile phase consisted of 0.1% acetic acid in water (mobile phase A; 10%), and MeOH (mobile phase B; 90%), utilizing an isocratic elution at a total flow rate of 0.25 mL/min. The retention time of MP-1 was 1.9 min and 4.5 min for PL-3. The method incorporated an additional 2.1 min after the final analyte peak bringing the total run time to 6.0 min. No interference from endogenous components were found in the biological matrix at MP-1 or the IS retention time (Figure 2).

### **3.2. Plasma and tissue sample preparation and liver S9 fraction sample preparation**

To optimize sample preparation, protein precipitation, liquid–liquid extraction and SPE methods were evaluated. The final SPE method was selected to prepare plasma and tissue samples due to its high extraction recovery. By comparing the SPE rate with various organic washing and eluting solvents, MeOH was finally selected as a reliable eluting solvent for SPE because it had good recovery with no matrix effect [19, 20]. The extraction method showed reproducible and consistent recovery at all the evaluated concentrations in plasma and tissue samples.

### **3.3. Assay validation**

#### **3.3.1. Selectivity and Sensitivity**

To analyze the specificity of the method, blank extracted plasma and tissue homogenate was analyzed for potential interferences at the retention times of 1.9 min (MP-1) and 4.5 min (IS). There was no significant interference or co-eluting peaks that were > 20% of the analytes area at the LLOQ level and no co-eluting peaks > 5% of the area of IS were observed, meeting the acceptance criteria and indicating the specificity of the method.

The LLOQ for MP-1 was determined to be 0.2 ng/ml. The intra-run precision at the LLOQ plasma samples containing MP-1 was 10.8%. The intra-run accuracy at the LLOQ plasma samples was 7.3%. These data are tabulated in (Table 2).

### 3.3.2. Calibration curve and linearity

The MP-1 calibration curve was linear over the range of 0.2 to 500 ng/mL (Figure 3). The correlation coefficient of determination ( $r^2$ ) was greater than 0.988.

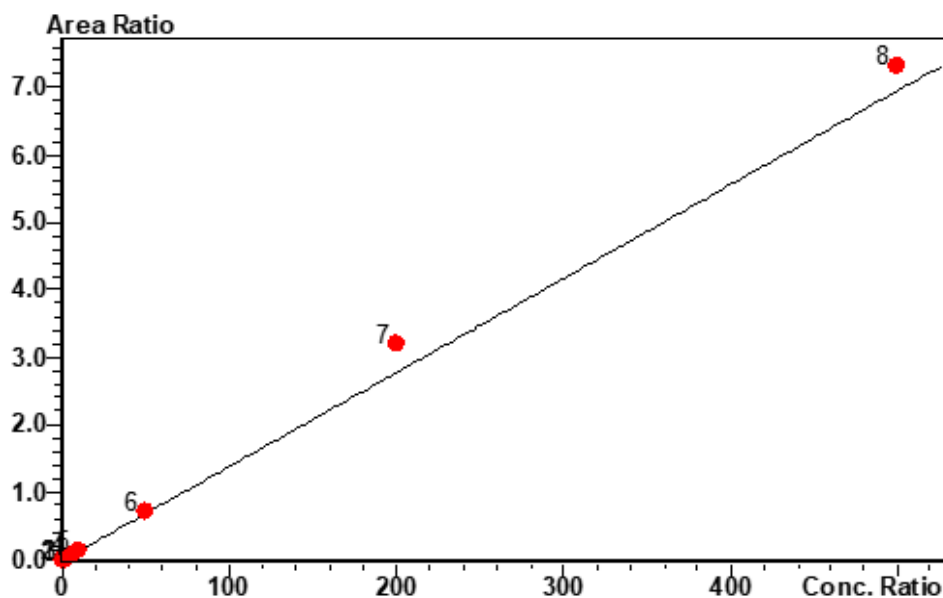


**Figure 2: MP-1 calibration curve and linearity.** Linear calibration fit for MP-1 of concentration range of 0.2 to 500 ng/mL,  $r^2= 0.988$  and %RSD= 9.97.

### 3.3.3. Carry-over

In order to assess carry-over, blank samples (running buffer only) were analyzed immediately after running HQC samples. No significant peaks,  $\geq 20\%$  LLOQ, were observed. Thus, it was concluded that carry over was negligible in the current method ( $<5\%$  of LLOQ).

### 3.3.4. Accuracy and precision

Intra-day accuracy and inter-day precision for MP-1 was assessed at four different concentrations in mouse plasma LLOQ (0.2 ng/mL), LQC (0.6 ng/mL), MQC (100 ng/mL) and HQC (375 ng/mL) levels. The accuracy and precision are listed in Table 2. The %RSD of precision values ranged from 1.4 to 13.6%, indicating acceptable assay precision. The accuracy of the quantitative analysis of the compounds was varied from -13.4- 7.3%, within the acceptance limits at all concentration levels.

Nominal Conc. (ng/mL)	Accuracy		Precision	
	%Bias intra-assay	%Bias inter-assay	%RSD intra-assay	%RSD inter-assay
LLOQ (0.2 ng/mL)	7.3	4.8	10.8	8.3
LQC (0.6 ng/mL)	3.9	-2.7	4.4	12.9
MQC (100 ng/mL)	-4.7	-14.0	1.4	13.6
HQC (375 ng/mL)	-13.4	-12.0	5.7	4.4

**Table 2: MP-1 accuracy and precision.** Intra-assay and inter-assay accuracy and precision of MP-1 in plasma (n = 6).

### 3.3.5. Recovery and matrix effect

Analyte recovery for MP-1 and IS from spiked plasma samples was calculated using three control samples (LQC – 0.6 ng/mL, MQC – 100 ng/mL and HQC – 375 ng/mL). The % extraction mean recovery for MP-1 in LQC, MQC and HQC was 95.8±2.6, 89.1.0 ±10.6 and 90.8±3.4%, respectively. The mean recovery of all QC levels was > 90%, whereas the mean recovery of IS was 87.3 ± 3.8%. The matrix effect was negligible and within the acceptable ± 15%. (Table 3)

<b>Nominal Conc. (ng/mL)</b>	<b>% Extraction recoveries (Mean ± S.D, n=3)</b>	<b>% Matrix Effect (Mean ± S.D, n=3)</b>
LQC (0.6 ng/mL)	95.8±2.6	103.7±8.6
MQC (100 ng/mL)	89.1±10.6	90.5±4.9
HQC (375 ng/mL)	90.8±3.4	99.6±7.6
Internal standard (IS) (0.5 ng/mL)	87.3±3.8	105.1±11

**Table 3: Recovery and matrix effect.** Assessment of the recovery and matrix effect of MP-1 in mouse plasma, (Mean ± S.D, n=3).

### 3.3.6. Stability

Stability of MP-1 was assessed by several means including 4 hr bench-top at room temperature 21 °C, three freeze-thaw cycles, autosampler stability for 24 hr at temperature of 4 °C, and long term stability for 12 months frozen -80 °C, MP-1 showed no appreciable instability as concentrations were within the accepted ±15% standard (Table 4).

Nominal Conc. (ng/mL)	Measured mean conc. (ng/mL)	% Accuracy
<b>Autosampler stability 4 °C, Mean ± S.D, n=3.</b>		
LQC (0.6 ng/mL)	0.515 ± 0.107	85.8±17.8
MQC (100 ng/mL)	102.8±9.5	102.85±9.45
HQC (375 ng/mL)	340.6±12.8	90.8±3.4
<b>Bench-top stability 21 °C, Mean ± S.D, n=3.</b>		
LQC (0.6 ng/mL)	0.57±0.03	94.2±4.9
MQC (100 ng/mL)	114.8±2.5	114.9±2.6
HQC (375 ng/mL)	386.5±15.2	103±4
<b>Freeze-thaw stability -80 °C, up to 3 Cycle, Mean ± S.D, n=3.</b>		
LQC (0.6 ng/mL)	0.67 ± 0.06	108.6 ± 8.9
MQC (100 ng/mL)	102.8 ± 11.95	101.4 ± 10
HQC (375 ng/mL)	366.3 ± 44.9	97.7 ± 11.96
<b>Long term stability -80 °C, 12 months, Mean ± S.D, n=3.</b>		
LQC (0.6 ng/mL)	0.61± 0.02	100.3 ± 4.1
MQC (100 ng/mL)	92.40 ± 7.92	92.4 ± 7.9
HQC (375 ng/mL)	383.69± 79.94	101.8 ±13.5

**Table 4: Stability of MP-1.** stability was tested in mouse plasma at different storage conditions, (Mean ± S.D, n=3).



### 3.3.7: Dilution integrity

The dilution integrity of the samples was ensured by diluting QC samples above the upper limit of quantification (ULOQ) with like matrix to bring to within quantitation range 0.2- 500 ng/ml. The mean analyzed value of all diluted samples is within 15% of nominal concentration, with precision of the replicates  $\pm 15\%$  coefficient of variation (data not shown).

### 3.3.8. Solubility of MP-1

The solubility of MP-1 in phosphate buffer (pH 7.4) was approximately 50  $\mu\text{g}/\text{mL}$  (Mean  $\pm$  S.D 51.19 $\pm$ 2.11  $\mu\text{g}/\text{mL}$ ).

## 3.4. *In vitro* studies

### 3.4.1. Gastrointestinal Stability of MP-1

The stability of the analyte was evaluated at gastrointestinal pH 1.2 and 6.8, as well as at physiological pH 7.4 using phosphate buffer. MP-1 was found to be stable with >99% parent remaining after 1h in SGF, pH 1.2, and 2 h of incubation in the other tested pH conditions (6.8 and 7.4). (Fig. 4)

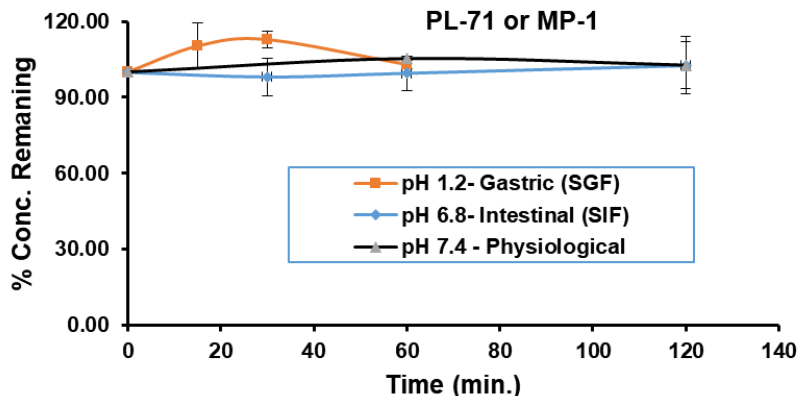


**Figure 3: Gastrointestinal Stability of MP-1.** MP-1 stability following a 2 hr incubation in buffer pH 7.4, SIF pH 6.8, SGF pH 1.2.

### 3.4.2. The blood to plasma ratio (Kb/p)

The blood:plasma (Kb/p) ratio was determined for MP-1 at a concentrations of 1  $\mu$ M (325 ng/mL). The Kb/p ratio was 0.40, 0.68 and 0.63 after 0, 30- and 60-min incubations at 37  $^{\circ}$ C (Table 5).

Time (min)	Blood Conc.	Plasma Conc.	Kb/p
	Mean (ng/ml) $\pm$ S.D	Mean (ng/ml) $\pm$ S.D	
0	294.1 $\pm$ 11.1	727.73 $\pm$ 49.16	0.40
30	490.7 $\pm$ 83.0	725.84 $\pm$ 157.67	0.68
60	490.8 $\pm$ 29.8	781.54 $\pm$ 24.53	0.63

**Table 5: The value MP-1 the blood to plasma ratio (Kb/p).** MP-1 concentration in blood and plasma, (Mean  $\pm$  S.D, n=3).

### 3.4.3. Plasma Protein Binding

MP-1 was highly bound (>95%) to mouse plasma proteins at both 1  $\mu$ g/ml and 10  $\mu$ g/ml concentrations. MP-1 was stable in mouse plasma following a 5 hr incubation (Table 6). There was no binding of MP-1 to the dialysis membrane (data not shown).

Nominal Conc. ( $\mu$ g /mL)	% Plasma Protein Bound $\pm$ S.D
MP-1 (1 $\mu$ g/ml)	99.96 $\pm$ 0.03
MP-1 (10 $\mu$ g/ml)	99.97 $\pm$ 0.02

**Table 6: MP-1 Plasma Protein Binding.** Plasma protein binding in mouse plasma (Mean  $\pm$  S.D values for MP-1, n=3).

### 3.4.4. In vitro metabolic stability in microsomes

*In vitro* metabolic stability of MP-1 was investigated using mouse, rat, and human liver microsomes. The time-dependent metabolic depletion of MP-1 in the interspecies microsomes is shown in Figure 5a. The *in vitro*  $t_{1/2}$  of MP-1 was 15.64  $\pm$  0.46, 18.1 $\pm$ 3.73, 27.47 $\pm$ 2.68 min in

mouse, rat, and human, respectively. The *in vitro* half-life ( $t_{1/2}$ ), intrinsic clearance ( $CL_{int}$ ) and *in vitro* hepatic clearance ( $CL_{int,H}$ ) of MP-1 in mouse, rat, and human microsomes are summarized in Table 7.

### 3.4.5. *In vitro* Metabolic stability in Mouse S9 Fraction

*In vitro* metabolic stability of MP-1 was investigated using mouse S9 fractions. The result of the metabolic stability study was expressed as the % parent remaining at different time points relative to the parent at 0 minutes (100% parent) (Figure 5a, b). The *in vitro*  $t_{1/2}$  of MP-1 was  $4.9 \pm 0.2$  min and  $CL_{int}$  of  $142.3 \pm 5.6$ .  $CL_{int}$  was calculated using the MP-1 depletion over time from initial substrate concentration of  $1\mu\text{M}$  (Table 7). Positive controls utilizing testosterone, 7-HC and diclofenac were within the acceptable in-house limits.

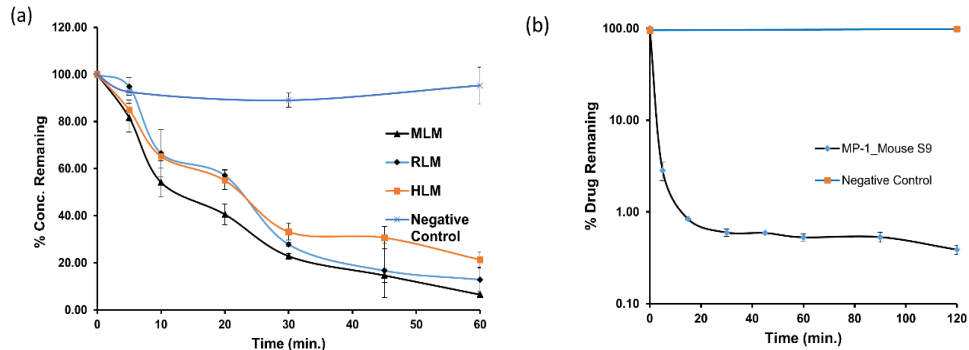


**Figure 4: Figure 4: MP-1 *in vitro* metabolic stability in microsomes.** Time-dependent metabolic depletion (% turnover or amount of drug remaining vs. incubation time) of MP-1 in microsomes and mouse S9 fraction (a) Interspecies microsomal metabolic stability of MP-1 in presence of NADPH and absence of NADPH as a negative control (b) mouse S9 metabolic stability of MP-1 in presence of NADPH and absence of NADPH as a negative control. Data shown as mean  $\pm$  S.D (n=3)

Parameters	MLM	RLM	HLM	Mouse S9
$t_{1/2}$ (min)	15.64 ± 0.46	18.1 ± 3.73	27.47 ± 2.68	4.9 ± 0.2
CL <sub>int</sub> (μL/min/mg protein)	88.72 ± 2.66	80.01 ± 16.5	50.99 ± 5.25	142.3 ± 5.6
CL <sub>int,H</sub> (mL /min/ kg body wgt)	479.07 ± 14.36	288.02 ± 59.41	81.58 ± 8.39	N/A

**Table 7: *In vitro* Metabolic stability in Mouse S9 Fraction.** MP-1 estimates for CL<sub>int</sub>,  $t_{1/2}$  and CL<sub>int,H</sub> in mouse (MLM), rat (RLM) and human (HLM) liver microsomes, and mouse S9, (Mean ± S.D, n=3).

### 3.4.6. Metabolite identification

Mouse S9 fraction samples were run in a 35 min gradient method using LC-MS/MS in positive and negative electrospray ionization (ESI) mode. Each peak, retention time and precursor ion peak [M-H]<sup>-</sup> was recorded and structural information was collected by fragmentation of all precursor ions. The mass of each predicted metabolite was used to generate post-acquisition extracted ion chromatograms (EICs).

The parent compound MP-1 was detected as a de-protonated molecular ion [M-H]<sup>-</sup> with a retention time of 25.39 min (Figure 6a). Two metabolites were identified based on their LC/MS data and putative structure via possible biotransformation, precursor ion, and retention times (Figure 7) and tabulated in Table 8. These results identify glucuronidation as the major metabolic pathway for MP-1.

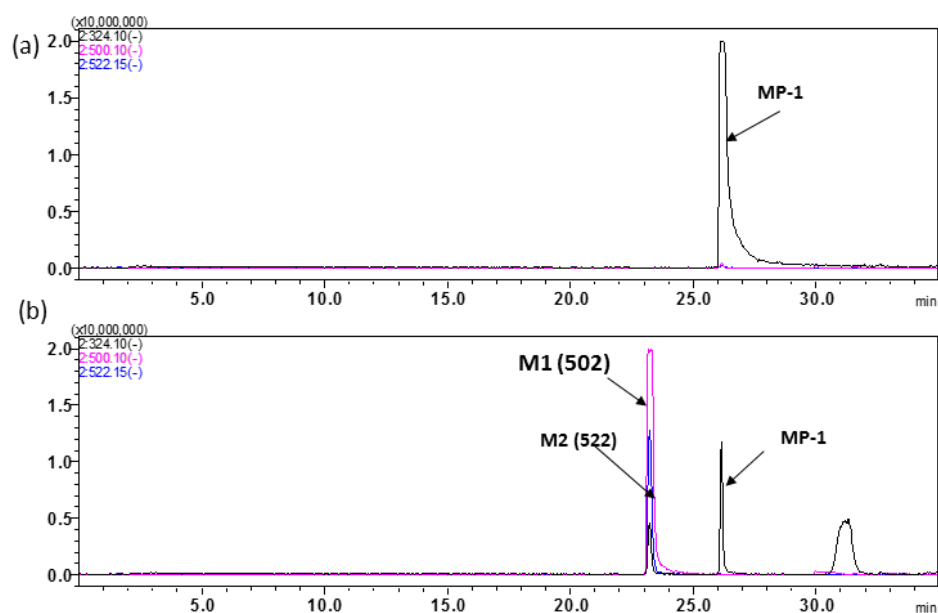


**Figure 5: MP-1 Metabolite identification.** Representative overly chromatogram of MP-1 and its metabolites under 35 min gradient chromatography.

Peak ID	Biotransformation	Mass Shift	Precursor ion (m/z)	Retention time (min)
	Parent (MP-1)	0	324.10	26.7
M1	Glucuronidation	176	500.12	23.0
M2	Unknown	198	522.15	23.0

**Table 8: MP-1 metabolites chromatogram summary.** MP-1 metabolites biotransformation, mass shift, precursor ion and retention time.

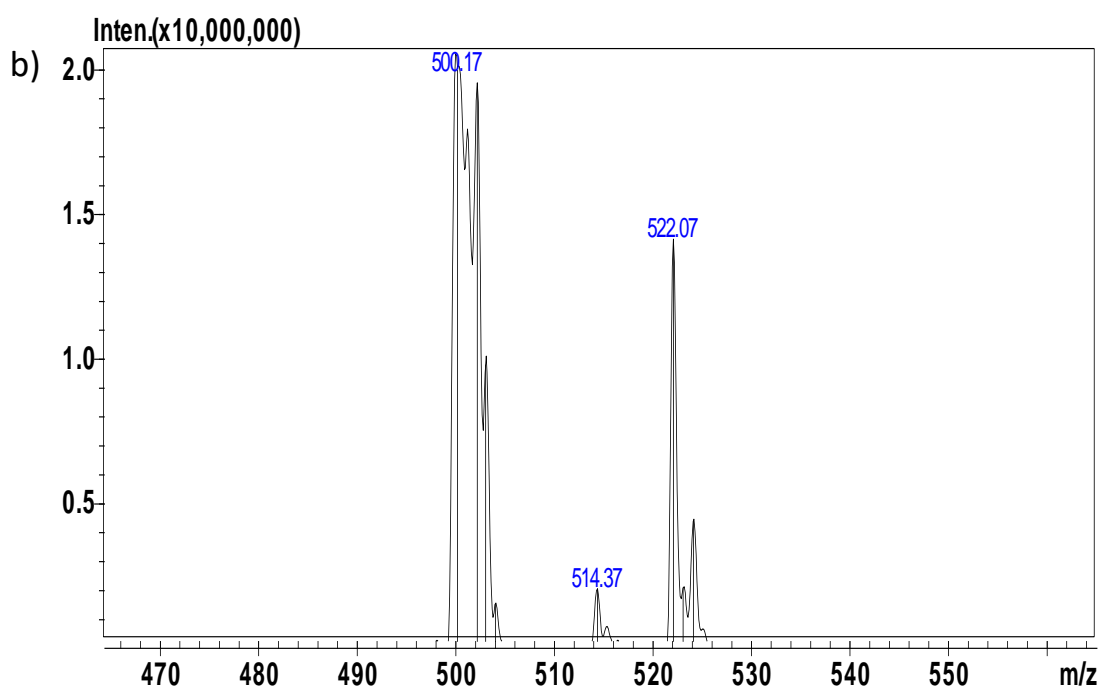
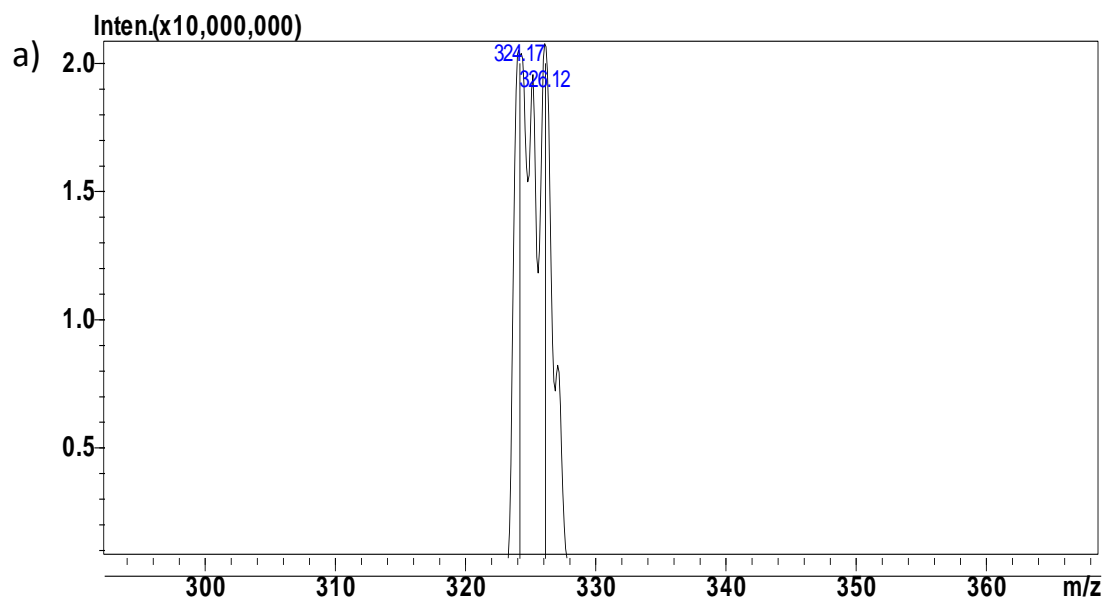


**Figure 6: MP-1 metabolites chromatogram:** a) Precursor ion spectra of MP-1 b) MP-1 metabolite in negative ESI mode, [M-H]<sup>-</sup> 324.10 and 500.10, respectively.

### 3.5. *In vivo* pharmacokinetic studies.

#### 3.5.1. Pharmacokinetic study

The developed and validated LC-MS/MS method was successfully applied to MP-1 pharmacokinetics and tissue distribution studies, following a single 15 mg/kg oral dose of MP-1 to Female BALB/c mice. The blood concentration vs. time profile for the MP-1 and its metabolites is shown in Figure 8.

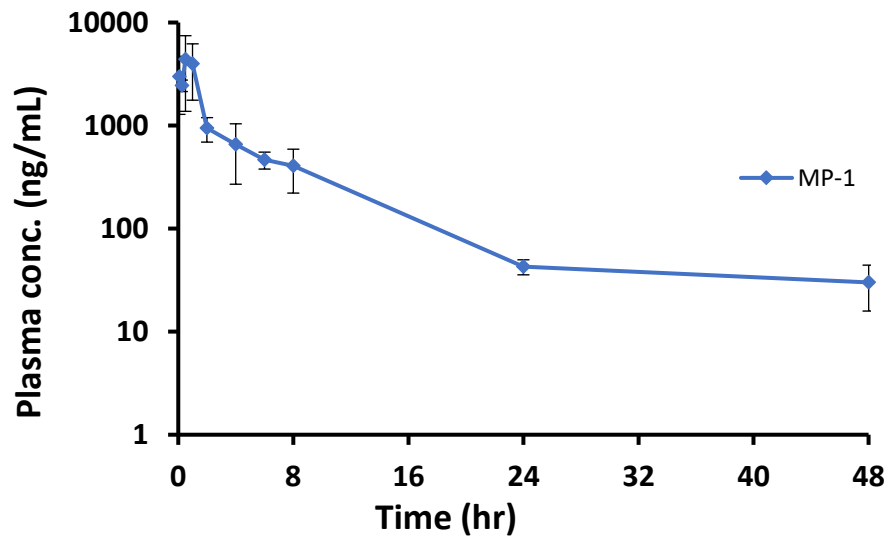


**Figure 7: The blood concentration vs. time profile for the MP-1.** Plasma concentration-time profile after 15mg/kg oral administration of MP-1 (Mean  $\pm$  S.D, n=4).

Time (hr)	Mean plasma conc. (ng/mL)	S.D
0.08	2,990.2	1,705.6
0.25	2,452.1	313.7
0.50	4,412.7	3,038.8
1	3,985.7	2,222.2

2	943.2	251.6
4	655.3	385.4
6	465.8	87.1
8	405.9	184.5
24	42.7	7.1
48	30.1	14.2

**Table 9: MP-1 Plasma concentration**, after 15 mg/kg oral administration in mice (Mean  $\pm$  S.D, n=4).

Pharmacokinetic data was processed with Phoenix<sup>®</sup> 8.2 (Certara Corporation, Mountain View, CA) software simulating through non-compartmental analysis. The mean non-compartmental pharmacokinetic parameters are shown in Table 10. Following oral administration, MP-1  $C_{max}$  was  $4714.7 \pm 2343.5$  ng/mL at a mean  $T_{max}$  of 0.6 hr. MP-1  $t_{1/2}$  was  $9.2 \pm 1.7$  hr and Cl was  $1.1 \pm 0.3$  L/h/kg.

PK Parameters	Mean	S.D	SE	CV%
$C_{max}$ (ng/ml)	4714.7	$\pm 2343.5$	1171.8	49.7
$T_{max}$ (hr)	0.6	$\pm 0.4$	0.2	68.9
$t_{1/2}$ (hr)	9.2	$\pm 1.7$	0.9	18.7
$AUC_{0-\infty}$ (hr $\times$ ng/mL)	15367.8	5466.9	2733.4	35.6
$AUC_{0-last}$ (hr $\times$ ng/mL)	14951.7	$\pm 5357.2$	2678.6	35.8
$V_d$ (L/kg)	13.9	$\pm 4.3$	2.1	30.9
Cl (L/hr/kg)	1.1	$\pm 0.3$	0.2	31.6

**Table 10: Summary of MP-1 pharmacokinetic parameters**, Non-compartmental pharmacokinetic parameters of MP-1 after 15 mg/kg oral administration (Mean, S.D SE and CV%, n=4).



### 3.5.2. Tissue distribution study

Concentrations of MP-1 was detected in all studied tissues, with the concentration the highest in the liver at all time points evaluated. Concentrations of MP-1 were detectable at 48 hours in all tissues (Figure 9).

Time (hr)	Lung		Spleen		Kidney		Brain		Heart		Liver	
	Mean (ng/g)	S.D	Mean (ng/g)	S.D	Mean (ng/g)	S.D	Mean (ng/g)	S.D	Mean (ng/g)	S.D	Mean (ng/g)	S.D
2	1,036	338.	445.4	219.	1,432	715	100.1	50.	759	258.	5,613	1,941
	.2	0		9	.2	.8		8	.1	1	.8	.2
4	705.3	671.	236.3	126.	1,351	874	77.7	14.	433	331.	5,583	2,912
		4		8	.6	.8		9	.0	3	.3	.9
8	619.2	392.	206.6	145.	1,463	751	56.3	27.	376	187.	3,615	1,699
		5		2	.7	.2		5	.2	9	.3	.5
48	3.4	3.4	3.9	4.3	15.3	16.	2.5	2.4	7.6	5.3		
						3					30.6	26.6

**Table 11: MP-1 tissues concentrations.** Tissue concentrations (ng/g) in liver, lungs, heart, kidney, brain, and spleen after 15mg/kg oral administration of MP-1 in mice (Mean ± S.D, n=4).

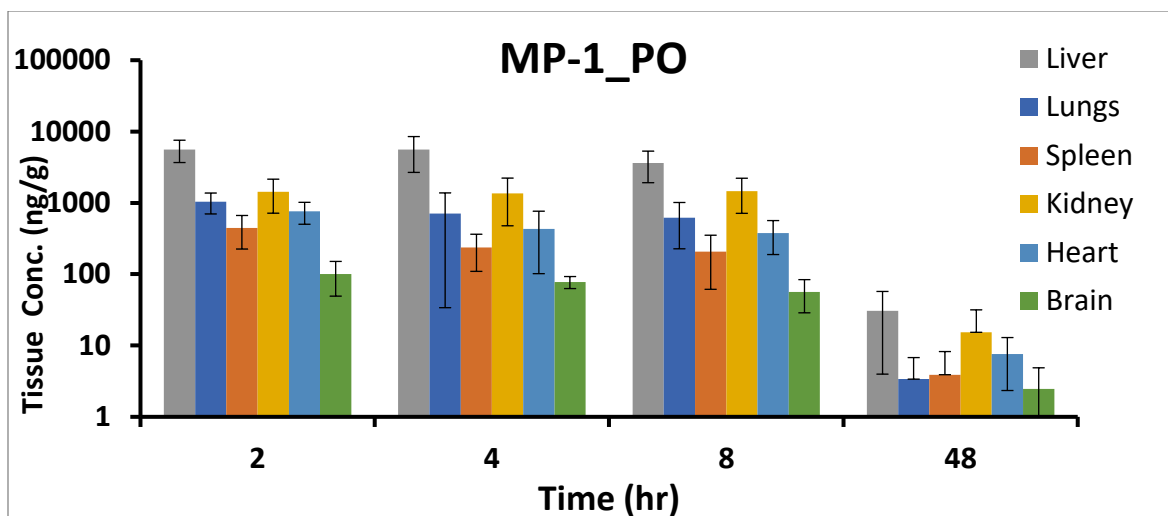


**Figure 8: MP-1 tissues concentrations.** Tissue concentrations (ng/g) at different time points in liver, lungs, heart, kidney, brain, and spleen after 15mg/kg oral administration of MP-1 in mice (Mean  $\pm$  S.D, n=4).

## CHAPTER 4:

### 4.1. Discussion

We successfully developed and validated a rapid, selective, and sensitive LC-ESI-MS/MS method for the quantitation of MP-1 in mouse plasma and tissues. The response was linear over the concentration range of 0.2-500 ng/mL with a correlation coefficient ( $r^2$ ) greater than 0.987 for all calibration curves. The method was validated according to FDA guidelines [12], showing accuracy and precision within the acceptance limits set forth by the FDA. The assay was sensitive with LLOQ of 0.2 ng/mL utilizing 100  $\mu$ L of plasma.

The optimized MS conditions utilized negative mode ESI<sup>-</sup> and resulted in lower background noise and acceptable sensitivity for the quantitation of MP-1 [19, 21]. LC separation was performed using reversed phase (C18) which is widely used by researchers for the relatively high organic content for solute interaction and, the better stability at both extremes of the working pH range. Because we used a reversed-phase stationary we were able to employ a polar mobile system consists of isocratic elution of 0.1% acetic acid in water (10% mobile phase A) and MeOH (90% mobile phase B). The use of the polar mobile system resulted in acceptable separation with high peak efficiency, peak symmetry and short total run time of 6 minutes making the method time efficient [19, 20, 22, 23].

Sample extraction and clean up was achieved using SPE. The developed SPE protocol was created while considering the drug physical-chemical properties and compatibility with the chosen LC method. The extraction method was reproducible with consistent high extraction recovery averaged of > 90% of MP-1 and > 85% of IS and negligible matrix effect [20, 22, 23].

The stability validation of MP-1 was determined under storage and use conditions, which emulate the laboratory handling conditions. MP-1 was stable under the tested conditions: 4 hr

bench-top at 21 °C, three freeze-thaw cycles, 24 hr, autosampler stability at 4 °C, and 12 months frozen -80 °C. Knowing the stability of MP-1 helps in selecting proper storage conditions and laboratory handling procedures to ensure high purity compound hence, more reproducible and reliable results[24]. Moreover MP-1 was found to be stable in gastrointestinal fluids with >99% parent remaining in SGIF, SIG and at physiological pH. MP-1 was highly bound (>95%) to mouse plasma proteins. The unbound drug concentration is considered to be pharmacologically and toxicologically active[14]. In addition, MP-1 mouse blood to plasma ratio (Kb/p) was <1 , indicating no significant partitioning of the compound into any of the specific component in the blood[25].

The metabolic stability of MP-1 was evaluated in mouse, rat, and human liver microsomes and mouse S9 fraction. MP-1 intrinsic clearance was  $88.72 \pm 2.66$ ,  $80.01 \pm 16.5$  and  $50.99 \pm 5.25$  ( $\mu\text{L}/\text{min}/\text{mg}$  protein) in mouse, rat, and human liver microsomes respectively. *In vitro* mouse S9 metabolic investigations exhibited rapid metabolic degradation with two metabolites being detected, with glucuronidation being the major metabolic pathway[18, 26].

The method was successfully applied to pharmacokinetic studies of the oral administration of MP-1. We found that MP-1 was rapidly absorbed with a  $T_{\text{max}}$  of 0.6 hours with a  $t_{1/2}$  of 9.2 hrs. MP-1 was found in the systemic circulation up to 48 hrs. In addition, MP-1 showed good penetration in all the tested tissues with the highest concentration in the liver and the lowest accumulation in the brain.

#### **4.2. Study limitations and future directions**

Following the pre-clinical studies investigating the biodistribution of MP-1, we found that MP-1 is rapidly distributed throughout the body. These studies provide the framework for future studies to design dosing regimens that achieve MP-1 concentrations associated with activity in

cell lines (i.e. the EC<sub>50</sub>). One of the limitations of this study is our drug concentrations represent total concentrations. Typically, free drug concentrations correlate with therapeutic effects better than total drug concentrations. Future studies will include an important parameter in precision dosing, which is drug tumor penetration, to bridging the gap between drug dose, free drug concentrations and the pharmacodynamic relation with tumor response.

## **5. Conclusion:**

In conclusion, we successfully developed and validated a rapid, selective, and sensitive LC-ESI-MS/MS method for the quantitation of MP-1 in mouse plasma and tissues. The assay was linear over the concentration range of 0.2-500 ng/mL. The LC-MS/MS bioanalytical method was validated according to FDA guidelines, showed acceptable selectivity, no significant matrix effects and acceptable accuracy and precision. In addition, we applied the validated method to the assessment of MP-1 *in vitro* and *in vivo* ADME properties in biological samples with nominal concentrations as low as 0.2 ng/mL.

## 6. Bibliography

1. Janoueix-Lerosey, I., *Neuroblastoma Pathogenesis*, in *Neuroblastoma: Clinical and Surgical Management*, S. Sarnacki and L. Pio, Editors. 2020, Springer International Publishing: Cham. p. 29-56.
2. Shohet, J. and J. Foster, *Neuroblastoma*. *Bmj*, 2017. **357**: p. j1863.
3. Matthay, K.K., et al., *Neuroblastoma*. *Nature Reviews Disease Primers*, 2016. **2**(1): p. 16078.
4. Aminzadeh, S., et al., *Energy metabolism in neuroblastoma and Wilms tumor*. *Transl Pediatr*, 2015. **4**(1): p. 20-32.
5. Cheung, N.K. and M.A. Dyer, *Neuroblastoma: developmental biology, cancer genomics and immunotherapy*. *Nat Rev Cancer*, 2013. **13**(6): p. 397-411.
6. Rickman, D.S., J.H. Schulte, and M. Eilers, *The Expanding World of N-MYC–Driven Tumors*. *Cancer Discovery*, 2018. **8**(2): p. 150-163.
7. Westermarck, U.K., et al., *The MYCN oncogene and differentiation in neuroblastoma*. *Seminars in Cancer Biology*, 2011. **21**(4): p. 256-266.
8. McGuire, T.R., et al., *Effects of novel pyrrolomycin MP1 in MYCN amplified chemoresistant neuroblastoma cell lines alone and combined with temsirolimus*. *BMC cancer*, 2019. **19**(1): p. 837-837.
9. Coughlan, D., et al., *Treatment and survival of childhood neuroblastoma: Evidence from a population-based study in the United States*. *Pediatric Hematology and Oncology*, 2017. **34**(5): p. 320-330.
10. Li, R., *Marinopyrroles: Unique Drug Discoveries Based on Marine Natural Products*. *Medicinal Research Reviews*, 2016. **36**(1): p. 169-189.
11. Doi, K., et al., *Discovery of Marinopyrrole A (Maritoclax) as a Selective Mcl-1 Antagonist that Overcomes ABT-737 Resistance by Binding to and Targeting Mcl-1 for Proteasomal Degradation*. *Journal of Biological Chemistry*, 2012. **287**(13): p. 10224-10235.
12. US FDA, D., *Bioanalytical method validation guidance for industry*. 2018.
13. Wang, J., et al., *Toward Oral Delivery of Biopharmaceuticals: An Assessment of the Gastrointestinal Stability of 17 Peptide Drugs*. *Molecular Pharmaceutics*, 2015. **12**(3): p. 966-973.
14. Lindup, W.E. and M.C. Orme, *Clinical pharmacology: plasma protein binding of drugs*. *British medical journal (Clinical research ed.)*, 1981. **282**(6259): p. 212-214.
15. Baarnhielm, C., H. Dahlback, and I. Skanberg, *In vivo pharmacokinetics of felodipine predicted from in vitro studies in rat, dog and man*. *Acta Pharmacol Toxicol (Copenh)*, 1986. **59**(2): p. 113-22.
16. Smith, R., et al., *Determination of microsome and hepatocyte scaling factors for in vitro/in vivo extrapolation in the rat and dog*. *Xenobiotica*, 2008. **38**(11): p. 1386-98.
17. Francis, B., et al., *Metabolite profiling study of propranolol in rat using LC/MS/MS analysis*. *Biomedical Chromatography*, 1999. **13**(5): p. 363-369.
18. Knights, K.M., et al., *In Vitro Drug Metabolism Using Liver Microsomes*. *Current Protocols in Pharmacology*, 2016. **74**(1): p. 7.8.1-7.8.24.
19. Krueve, A., *Influence of mobile phase, source parameters and source type on electrospray ionization efficiency in negative ion mode*. *Journal of Mass Spectrometry*, 2016. **51**(8): p. 596-601.
20. *Reversed Phase Liquid Chromatography*, in *Analytical Separation Science*. p. 159-198.
21. Liigand, P., et al., *Think Negative: Finding the Best Electrospray Ionization/MS Mode for Your Analyte*. *Analytical Chemistry*, 2017. **89**(11): p. 5665-5668.

22. Moldoveanu, S.C. and V. David, *Chapter 5 - Retention Mechanisms in Different HPLC Types*, in *Essentials in Modern HPLC Separations*, S.C. Moldoveanu and V. David, Editors. 2013, Elsevier. p. 145-190.
23. Sargent, M., *Guide to achieving reliable quantitative LC-MS measurements*. RSC analytical methods committee, 2013.
24. Blessy, M., et al., *Development of forced degradation and stability indicating studies of drugs—A review*. *Journal of Pharmaceutical Analysis*, 2014. **4**(3): p. 159-165.
25. Saha, A., et al., *Role of RBC Partitioning and Whole Blood to Plasma Ratio in Bioanalysis: A Case Study With Valacyclovir and Acyclovir*. *Mass Spectrometry & Purification Techniques*, 2017. **03**.
26. Beaudry, F., et al., *Metabolite profiling study of propranolol in rat using LC/MS/MS analysis*. *Biomed Chromatogr*, 1999. **13**(5): p. 363-9.